

# Study of in-medium $\omega$ meson properties in Ap, pA and AA collisions

S.Belogurov, M.Chumakov, S.Kiselev, Yu.Kiselev\*, V.Sheinkman

January 17, 2008

*Institute for Theoretical and Experimental Physics  
Moscow, Russia*

## Abstract

We propose to investigate the in-medium properties of the vector  $\omega$  mesons at normal nuclear density in Ap(pA) collisions and at higher density in AA collisions at ITEP accelerator facility TWAC. The using of the inverse Ap kinematics will permit us to study the  $\omega$  meson production in wide momentum interval included the not yet explored range of small meson momenta relative to the projectile nuclei where the mass modification effect in nuclear matter is expected to be most strong. The momentum dependence of the in-medium  $\omega$  meson width will be studied in the traditional pA kinematics. We intend to use the electromagnetic calorimeter for the reconstruction of the meson invariant mass by detecting the photons from the  $\omega \rightarrow \pi^0\gamma \rightarrow 3\gamma$  decay. The model calculations and simulations with RQMD generator show the feasibility of the proposed experiment. Available now intensity of the ion beams provides the possibility to collect large statistics and make decisive conclusion about the  $\omega$  meson properties at the density of normal nuclei. At the second stage of the investigation the  $\omega$  meson properties will be studied in AA collisions at higher density. The interpretation of these measurements will be based on the results obtained in Ap(pA) interactions. Further investigation of the in-medium properties of light and heavy mesons can be performed at ITEP and at GSI(FAIR) where higher ion energies will be accessible in near future.

---

\*e-mail address: yurikis@itep.ru

# Contents

|           |   |           |
|-----------|---|-----------|
| <b>1</b>  | <b>Physics motivaion</b>  | <b>3</b>  |
| <b>2</b>  | <b>Goal of the experiment</b>                                   | <b>4</b>  |
| <b>3</b>  | <b>Theoretical predictions</b>                                  | <b>4</b>  |
| <b>4</b>  | <b>Inverse and direct kinematics</b>                            | <b>5</b>  |
| <b>5</b>  | <b>Experimental arrangement</b>                                 | <b>7</b>  |
| 5.1       | Extracted ion and proton beams . . . . .                        | 7         |
| 5.2       | Projectiles and targets . . . . .                               | 8         |
| 5.3       | Photon detector . . . . .                                       | 8         |
| <b>6</b>  | <b>Study of the <math>\omega</math> meson in nuclear matter</b> | <b>8</b>  |
| 6.1       | In-medium $\omega$ meson mass . . . . .                         | 8         |
| 6.2       | In-medium $\omega$ meson width . . . . .                        | 11        |
| <b>7</b>  | <b>Simulations with RQMD event generator</b>                    | <b>13</b> |
| <b>8</b>  | <b>Background and its suppression</b>                           | <b>18</b> |
| <b>9</b>  | <b>Event trigger</b>  | <b>20</b> |
| <b>10</b> | <b>Event rate estimate</b>                                      | <b>20</b> |
| <b>11</b> | <b>Conclusion</b>   | <b>21</b> |
| <b>12</b> | <b>Further investigations at ITEP and GSI</b>                   | <b>22</b> |
| <b>13</b> | <b>Acknowledgments</b>  | <b>23</b> |

# 1 Physics motivation

The modification of the hadron properties in baryon environment is one of the important topics of contemporary strong interaction physics. This phenomenon has been predicted within various theoretical approaches such as QCD sum rules [1], chiral dynamics [2], relativistic mean-field [3] and quark-meson coupling model [4]. The recent review can be found in Ref. [5]. A hadron can change its properties such as mass and width once it is embedded into a baryon matter. This change is connected to the many body interactions of a hadron with surrounding nucleons. Whether a hadron is - in addition - also affected by QCD condensates and their in-medium change [1], [2], [6] is still a matter of debate. Nevertheless, the great interest in study of in-medium hadron properties is caused by the expectation to find the evidences of the chiral symmetry restoration. The investigation of the vector mesons is of special interest in this context. Theoretically, the possibility of the decrease in the mass of light vector mesons in matter was first pointed by Brown and Rho [2]. In their approach the masses of the vector mesons scale with quark condensate, i.e. drop with rising of baryonic density. The observation of this effect can be precursor phenomena of the transition of strongly interacting matter to the chirally symmetric phase. First experimental signal of this phenomenon was recently observed in [7]. Nambu and Jona-Lasino proposed the spontaneous breaking of the chiral symmetry as the fundamental mechanism for the creation of a mass of hadrons [8]. Recently, the in-medium change of the  $\omega$  mesons spectral function was proposed as a probe of higher order QCD four-quark condensate [9].

An evidence for a decrease of the  $\rho$  meson mass in heavy-ion collisions was obtained by the CERES collaboration at CERN [10] and later by the STAR collaboration at RHIC [11]. Since heavy-ion interaction is very complicated process in which the temperature and baryon density varies dramatically with time due to the formation and expansion of the "fireball", the interpretation of experimental data on nucleus-nucleus collisions is far from being simple. The above results have been found an explanation in terms of a shift  $\rho$  meson spectral function to a lower mass, as expected from the theory. However, even the calculations that just used the free radiation rates with their - often quite large - experimental uncertainties are compatible with the observation.

Therefore, it is useful to explore the reactions with elementary probes ( $\gamma$ ,  $\pi$ ,  $p$ ) since sizeable - about 20% - medium effects were predicted already at the density of ordinary nuclei [2], [12], [13]. The advantage of the investigations of the reactions on nuclei is related to the fact that they proceed in the nearly cold static nuclear matter and thus the colliding system is much better under control. Indeed, the first signals for lowering of the  $\omega$  meson mass at normal nuclear matter density were recently observed in the  $\gamma A$  [14] and  $pA$  [15] reactions. However, the critical analysis [16] shows that data of the experiment [14] are compatible with normal  $\omega$  mass and an enlarged width. In contrast to the conclusion [15]

the preliminary results of CLAS collaboration on the photoproduction of  $\rho$  and  $\omega$  mesons [17] also evidence for no shift in the mass. Now there are exist only first estimates of the  $\omega$  meson width in matter [14], [18]. Thus, the available now experimental information does not allow to draw the final conclusion about the change of the  $\omega$  meson properties in nuclear matter of normal density. It should be stressed that the indications for the decreasing of the  $\omega$  meson mass in both experiments [14], [15] have been found for the mesons with low momenta relative to the surrounding nuclear matter. Therefore, next generation of experiments need to addresses the issue of momentum dependence of medium effects. We suggest to explore the momentum dependence of the in-medium mass and width of the  $\omega$  meson using the ion and proton beams of the ITEP accelerator facility TWAC [19].

The investigation of in-medium meson modification addresses the fundamental problems of strong interaction physics and is one of the hot current topics nowadays. The experiments with photon, pion, proton and ion projectiles are planned in wide collision energy range from a few GeV (GSI, JLAB, JINR, COSY, SPRING-8, ITEP) till TeV (RHIC, LHC).

## 2 Goal of the experiment

The goal of the proposed experiment is the investigation of the  $\omega$  meson properties at normal nuclear density  $\rho_0 = 0.17fm^{-3}$  in nucleus-proton collisions and at higher density in nucleus-nucleus collisions. The experiment aims at the study of vector mesons with low momentum relative to baryonic environment where the in-medium mass modification is expected to be most strong as well as at the study of high momentum range which is sensitive to the in-medium  $\omega$  meson width.

## 3 Theoretical predictions

All information about the intrinsic properties of a meson is encoded in its spectral function  $S(M)$  which can be written in non-relativistic Breit-Wigner form. In free space:

$$S(M) = (\Gamma_0/2)^2 / [(M - M_0)^2 + (\Gamma_0/2)^2], \quad (1)$$

where  $\Gamma_0$  and  $M_0$  stand for a meson width and pole mass, correspondingly.

Due to the interaction with surrounding nuclear medium the meson acquires a self-energy  $\Sigma$  which is related to the nuclear optical potential  $U$  as [20]:

$$\Sigma/2E = U = ReU + iImU, \quad (2)$$

where  $E$  is the total meson energy.

The meson spectral function in nuclear medium is read:

$$S(M) = [(\Gamma_0/2) + (\Gamma^*/2)]^2 / [(M - M_0 - M^*)^2 + [(\Gamma_0/2) + (\Gamma^*/2)]^2]. \quad (3)$$

Two extra terms,  $M^*$  and  $\Gamma^*/2$ , which describe the shift of the meson pole mass and the increase of its width in matter, are related to the nuclear optical potential  $U$  as follows [20]:

$$M^* = \text{Re}U; \Gamma^*/2 = -\text{Im}U; \quad (4)$$

The pole mass and width of the  $\omega$  meson in free space (vacuum) are  $M = 782$  MeV and  $8.4$  MeV, correspondingly. Most theoretical investigations predict the dropping of the in-medium  $\omega$  meson mass by 20-140 MeV [21] at normal nuclear density. However, there have also been suggestions for a rising mass [22] or even a structure with several peaks [23]. At the same time there seems to be a general agreement that in-medium  $\omega$  width is within the range from 20 MeV to 60 MeV [24] at the density  $\rho = \rho_0$ . Thus, it is expected that the  $\omega$  meson in matter survives as a quasiparticle and can be observed as a structure in the  $\omega$  mass spectrum. In principle, both dilepton and  $\pi^0\gamma$  invariant mass spectra can be used for the study of modification effects. The advantage of the dilepton decay channel is related to the fact that leptons are almost undistorted by the final state interactions. However, the  $\omega$  signal in the dilepton mode is rather weak ( $BR(\omega \rightarrow e^+e^-) \approx 7.1 \times 10^{-5}$ ) and is always accompanied by a comparatively large background from  $\rho^0 \rightarrow e^+e^-$  decays. The  $\omega \rightarrow \pi^0\gamma$  decay has a branching ratio  $8.9 \times 10^{-2}$  what is 3 orders of magnitude higher. Furthermore, the competing  $\rho \rightarrow \pi^0\gamma$  channel has a branching ratio which is a factor  $10^2$  smaller. By these reasons the  $\omega \rightarrow \pi^0\gamma$  decay mode can be considered as an exclusive probe to study the  $\omega$  meson properties in matter. The disadvantage of this channel is a possible rescattering of the  $\pi^0$  within the nuclear medium which would distort the deduced  $\omega$  invariant mass distribution. However, as it was shown in Refs. [25], [26] the above distortion effect can be significantly decreased by applying an appropriate cut on the pion kinetic energy.

## 4 Inverse and direct kinematics

The  $\omega$  meson invariant mass spectrum has two components which correspond to the decay 'inside' and 'outside' the nucleus. Only vector mesons decaying 'inside' nuclei can be used for an identification of the in-medium  $\omega$  mass. This imposes the kinematical condition that the decay length of the vector meson should be less than nucleus size. It implies that the  $\omega$  meson should be produced with small momentum (velocity) relative to the nuclear matter rest frame. The study of low momentum  $\omega$  mesons production in the inverse Ap kinematics [27] has several important advantages over the study in the direct pA kinematics. First, as it follows from the Lorentz transformation, a slow particles in a projectile nucleus

system appear to be fast in the laboratory (in the target proton rest frame) and become convenient for the detection. At beam energy of 4 AGeV all the  $\omega$ 's produced in full solid angle with momenta less than 0.3 GeV/c relative to the projectile nucleus rest frame will be concentrated in the laboratory inside narrow cone of less than  $\pm 5^\circ$  and the momentum range from 2.8 till 5.9 GeV/c. The produced mesons which are almost at rest inside the incident nucleus ("comovers") have the laboratory momenta around of 4 GeV/c. Due to the decrease of the production cross section with laboratory  $\omega$  meson momentum the main contribution to the  $\omega$  yield comes from the momentum interval of 2.8 - 4.0 GeV/c. These events will be observed in small phase space  $dPdcos\theta$  in the laboratory resulting in significant increase of the forward production cross section as compared to one in pA reactions. That can be easily understood because experimentally observed *non-invariant double differential cross sections* measured in the direct (pA) and inverse (Ap) kinematics are related as:

$${}^{Ap}(d^2\sigma/dPdcos\theta) = {}^{Ap}(P^2/E)^{pA}(E/P^2)^{pA}(d^2\sigma/dPdcos\theta). \quad (5)$$

One can see that the factor  ${}^{pA}(E/P^2)$  grows strongly with lowering of the  $\omega$  meson momentum while the factor  ${}^{Ap}(P^2/E)$  changes rather smoothly. For example, at the momentum  ${}^{pA}P = 0.25$  GeV/c the product of two above factors is equal to 37. The photons from the decay  $\omega \rightarrow \pi^0\gamma \rightarrow 3\gamma$  are distributed inside more wide cone as compared to parent mesons, however the coverage of the angular interval  $5^\circ - 25^\circ$  - which corresponds to the solid angle of less than 9% of  $4\pi$  - permits to collect significant part of the useful events depending on the detector layout (see section 7).

Second, the mean free pass of the proton in nuclear matter is as small as 2 fm and therefore the  $\omega$  mesons are predominantly created inside the front layers of a projectile nucleus. Since the forward produced  $\omega$ 's in the momentum range 2.8-4.0 GeV/c have the laboratory velocities which are less than ones of the surrounding nucleons, the produced mesons move in the direction opposite to the ion beam direction and then decay in more dense inner layers of a nucleus. That is of great importance because the strength of the medium effects increases with local nuclear density.

Third advantage of the inverse kinematics is an increase of the detected photons energies because they are emitted by relativistic  $\omega$  and  $\pi^0$ . For example, the  $\pi^0\gamma$  decay in transverse direction of the  $\omega$  carrying the momentum of 4 GeV/c results in emission of the photon of energy 2 GeV and  $\pi^0$  of energy 2.1 GeV followed by the pion decay to two photons of 1 GeV energy. The above energies exceed the photon energies from the  $\omega \rightarrow \pi^0\gamma$  decay at rest (0.38 GeV for the  $\gamma$  from  $\omega$  and 0.19 GeV for the  $\gamma$ 's from  $\pi^0$ ) by a factor of about 5. That results in more precise measurement of the photon energy leading to more narrow width of the signal in the invariant mass spectrum and hence improved signal to background ratio. At last, only moderate momentum resolution in the laboratory is required

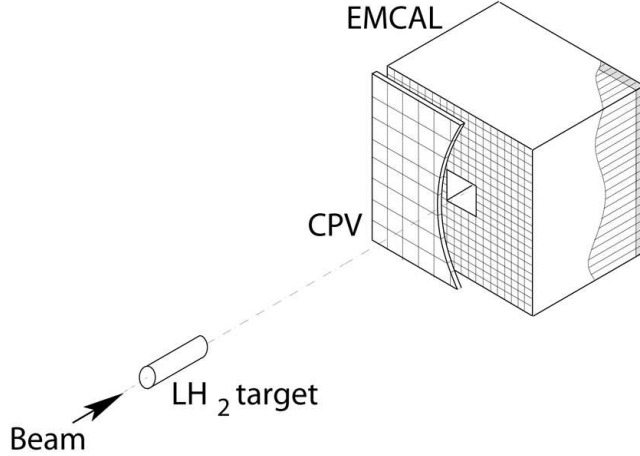


Figure 1: Sketch of the experimental set-up

for the rather precise determination of the  $\omega$  momentum relative to the projectile nucleus because the momentum range of interest 2.8-4 GeV/c in the laboratory corresponds to the interval 0-0.3 GeV/c in the nucleus frame of reference.

In contrast with in-medium  $\omega$  meson mass the value of its width is expected to be deduced from the analysis of the production of fast mesons relative to the baryonic matter. It is well known that high momentum mesons can be abundantly produced in the pA interactions. Thus, the combination of the Ap and pA measurements provides the possibility to study both  $\omega$  meson mass and width in nuclear matter.

## 5 Experimental arrangement

### 5.1 Extracted ion and proton beams

The experiment will be carried out with ion and proton beams of TWAC extracted in the inner hall of the accelerator. Expected extraction efficiency is of 50%. Two dipole and two pairs of quadrupole magnets serve for the deflection and focusing of the beams onto the target. The sketch of the experimental set-up is shown in Fig. 1. The ions (or protons) which do not interact in the target pass through the central hole of the electromagnetic calorimeter (EMCAL) and then directed to the downstream beam-dump located in the inner hall or thick concrete wall of the accelerator. That prevents the environment from the radiation pollution.

## 5.2 Projectiles and targets

The projectile Ta, Cu, Al and C ions will be used for the investigations of the in-medium  $\omega$  meson mass while the projectile protons will be used for the exploration of the  $\omega$  width in the nuclear matter. The proton runs will also permit us to study the EMCAL performance and calibrate the invariant mass scale by measurements of the reactions like  $p + A \rightarrow \pi^0 + X$ ,  $p + A \rightarrow \eta + X$  and  $p + A \rightarrow \omega + X$ .

The liquid hydrogen ( $LH_2$ ) target of 2% interaction length (12 cm) will be produced by the cryogenic division of Petersburg Nuclear Physics Institute (PNPI) and by the ITEP specialists. We plan to use the simple foil targets (Be, Al, Cu, Ag and Ta) for the pA and AA measurements.

## 5.3 Photon detector

The ring-like electromagnetic calorimeter with total area of  $0.64 \text{ m}^2$  will be located at the distance of 1 m behind the target. We intend to use the EMCAL based on the PbWO cells  $20 \times 20 \text{ mm}^2$  size with avalanche photodiode or photomultiplier readout. The energy and spatial resolution of the cell are  $\sigma/E = 2\% \sqrt{E} + 1\%$  and  $\sigma_x = \sigma_y = 6 \text{ mm}$ , respectively. The total number of cells is 1400. In front of each cell (or group of cells) the 5 mm thick plastic scintillator with photodiode readout will be mounted for the detection of charged particles. Due to the moderate charge ejectile multiplicity (see section 7) the number of CPV (Charged Particle Veto) counters is less than about 100. This array will be also used as a multiplicity detector offering the possibility to apply the cuts on the impact parameter of the collision.

# 6 Study of the $\omega$ meson in nuclear matter

## 6.1 In-medium $\omega$ meson mass

For the evaluation of the expected signal of in-medium  $\omega$  meson mass and width modification the calculations of the  $\omega$  meson production were performed in the framework of the folding model. The model takes properly into account both incoherent direct proton-nucleon and secondary pion-nucleon  $\omega$  meson production processes as well as internal nucleon momentum distribution (see for example [28]). The folding model describes the production, propagation and decay of the  $\omega$  meson inside a nucleus taking into account its four-momentum and local nuclear density. The calculations were performed for Ta, Cu, Al and C nuclei at initial energy of 4 AGeV.

We primary focus at study of the  $\omega$  mesons with low momentum in the projectile nucleus rest frame by two reasons. First, the strength of the 'inside' component of the  $\omega$  decay - which carries the information on the in-medium meson mass - obviously increases with lowering of a meson momentum. Second, the

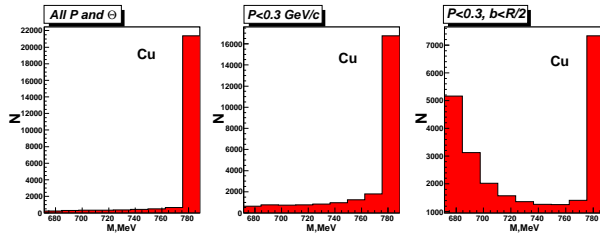


Figure 2:  $\omega$  meson mass spectra without and with the cuts on the meson momentum and collision impact parameter

in-medium  $\omega$  mass shift can depend on the meson velocity with respect to the surrounding nuclear matter (see discussion in [25]). The most strong effect is predicted to be manifest itself in the low momentum range. One can also expect that the low momentum  $\omega$  mesons can be captured by the nucleus which leads to the formation of the  $\omega$  - nucleus bound state [29], [5].

The  $\omega$  meson mass shift was introduced according to the local nuclear density  $\rho(r)$ :

$$M^* = ReU = \delta M_0 \rho / \rho_0, \quad (6)$$

where  $M_0$  stands for the  $\omega$  meson vacuum mass. The negative value of  $\delta = -0.12$  - in accordance with experimental observations [14], [15] - means that the  $\omega$  meson fills a strong attraction inside nuclear matter which is of about  $ReU = -90 MeV$  at nuclear saturation density  $\rho_0$ . In our calculations the nuclear density distributions were taken in two-parameter Fermi form.

The mass distribution of all  $\omega$ 's produced in Cu+p collisions at 4 AGeV is shown in the left panel of Fig. 2. The right peak corresponds to the decays 'outside' the nucleus and hence to the vacuum  $\omega$  meson mass while the left part of the distribution corresponds to the decays 'inside' the nucleus and contains the events with reduced meson masses.<sup>1</sup> The relative amount of events where the  $\omega$  decay at finite nuclear matter density is vanishingly small. The middle part of Fig. 2 presents the distribution for the  $\omega$  meson of momentum  $\leq 0.3$  GeV/c relative to the projectile nucleus frame of reference. The fraction of the 'inside' decays increases up to 1/3. The mass distribution for low momentum

<sup>1</sup>We refer a decay to the 'inside' component provided the local density  $\rho/\rho_0 > 0.05$ .

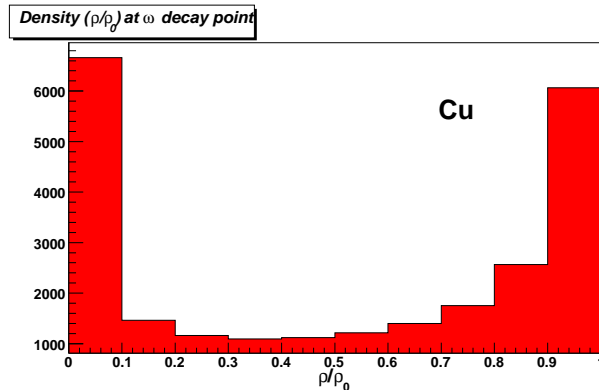


Figure 3: Nuclear density at the  $\omega$  meson decay point for  $P < 0.3\text{GeV}/c$  and  $b < R_{Cu}/2$

$\omega$ 's produced in the central collisions with the impact parameter  $b < R_{Cu}/2$  is shown in the right part of Fig. 2. One can see further drop of the vacuum peak accompanied by the enlargement of the 'inside' component up to  $2/3$ . The vacuum peak is still survived however it can be rather accurately subtracted from the observed mass spectrum as its width and pole position are well known.

The density distribution with the above cuts on the  $\omega$  momentum and the impact parameter is shown in Fig. 3. It is seen that significant part of low momentum mesons produced in the central collisions decays in dense layers of the nucleus. Note that the calculations within the folding model provide the possibility to estimate average nuclear density for the 'inside' decay component.

It should be mentioned that inelastic  $\omega$ -nucleus collisions, i.e., the processes  $\omega N \rightarrow \omega X$  result in slowing down of the  $\omega$  mesons and an enhancement of low momentum part of the spectrum. Moreover, one can expect that the range of low  $\omega$  momenta would be even further enhanced because the momentum transfer from such a meson to a nucleon would be very small. Hence, any such scattering processes are hindered by Pauli blocking. Both above effects are not included in the folding model calculations.

Thus, we conclude that the expected signal of the  $\omega$  meson mass shift is strong enough to be observed experimentally. The proposed detector layout will permit us to collect sizeable statistics on the  $\omega$  meson production with low momenta relative to the surrounding nuclear matter (see section 10) and study the momentum dependence of the predicted effect.

## 6.2 In-medium $\omega$ meson width

The straightforward determination of the in-medium  $\omega$  meson width from the shape of the spectral function is hardly possible because the rescattering of the pion would change its kinematical parameters which results in distortion of the observed invariant mass peak. The authors of Ref. [20] have proposed the alternative method to study the  $\phi$ -meson width in the nuclear medium - by an attenuation measurements of the  $\phi$  meson flux in photonuclear reactions on different nuclear targets. This method is based on the well known connection of the particle absorption in nucleus with the imaginary part of the respective nuclear optical potential (see Eq.4). The method proposed in Ref. [20] was applied by Muehlich and Mosel to the  $\omega$  photo-production [30]. The flux of  $\pi^0\gamma$  pairs which escape a nucleus had been calculated within the Boltzmann-Uehling-Uhlenback (BUU) coupled-channel transport approach. As a measure of the  $\omega$  width in nuclei the authors of Ref. [30] used the so-called nuclear transparency ratio:

$$T_A = \sigma_{\gamma A \rightarrow V X} / A \sigma_{\gamma N \rightarrow V X}, \quad (7)$$

i.e. the ratio of the inclusive  $\omega$  photo-production cross section on nucleus divided by  $A$  times the same quantity on a free nucleon. It can be interpreted as the probability of the  $\omega$  meson to get out of the nucleus. The loss of flux is obviously related to the absorptive part of the  $\omega$ -nucleus potential and thus to the  $\omega$  width in nuclear medium. It was shown that the  $A$ -dependence of production cross sections significantly differs from that expected in the case when there are no medium effects on the  $\omega$  width. Similarly, the valuable information about the  $\omega$  width in the matter can be obtained from the analysis of  $A$ -dependence of  $\omega$  meson production cross section in proton-induced reactions.

The  $\omega$  width in nuclear matter is defined by Eq.3, where  $\Gamma_0$  is free meson width and the additional width  $\Gamma^*$  can be expressed according to Ref. [31]:

$$\Gamma^* = \gamma \{ \beta \sigma_{\omega N} \} \rho(r). \quad (8)$$

Here  $\beta$  is the relative velocity of nucleon and  $\omega$  meson,  $\gamma$  denotes the Lorentz factor for the transformation from nuclear rest frame to the  $\omega$  rest frame,  $\rho(r)$  stands for the local nuclear density. It is seen that in-medium  $\omega$  meson width depends on its velocity (momentum) relative to the nucleus rest frame. The total  $\omega N$  cross section in the free space  $\sigma_{\omega N}$  was adopted from the model [32]:

$$\sigma_{el} = [5.4 + 10 \exp(-0.6|\vec{q}|)] \text{ mb}; \quad (9)$$

$$\sigma_{in} = [20 + 4/|\vec{q}|] \text{ mb}; \quad (10)$$

The brackets in Eq.8 indicate an average over the Fermi motion of the nucleons. In Ref. [30] the  $\omega$  collision width was estimated as 37 MeV at nuclear saturation density for vanishing meson momentum.

Obviously, the discussed above  $\omega$  width calculated according the Eq. 8 with total  $\omega$ -nucleon cross section in the free space is only the estimate. According to Eg. 10 the inelastic cross section strongly increases with lowering of the  $\omega$  momentum. This holds as long as the momentum of the  $\omega$  meson is not small because Pauli blocking prevents the low energy  $\omega$ N interactions. The real  $\omega$ N cross section in the medium can differ from that in the free space. Indeed, the experiment on incoherent  $\phi$  photoproduction on Be, C, Al and Cu targets recently performed at SPring8 (LEPS) [33] have found an unexpectedly strong dependence of the loss of  $K^+K^-$  flux from the  $\phi$  decay on target mass number. The total in-medium  $\phi$ N cross section has been estimated by the authors as  $35_{-11}^{+17}$  mb using the Glauber-type multiple scattering theory. This value significantly differs from  $\sigma_{\phi N}^{tot}$  in the free space which is equal to 9-11 mb. One can expect similar effect for the  $\omega$  mesons.

Although a proton initial state interaction is rather strong, the  $\omega$  absorption is essential. For small angle  $\omega$  production the last effect can be taken into account by the Glauber eikonal factor which explicitly depends on the  $\omega$  meson width  $\Gamma^*$  [34]:

$$P = \exp\left[-\int_0^\infty dl \Gamma^*(p_\omega, \rho(r'))/\beta_\omega\right], \quad (11)$$

where  $\vec{r}' = \vec{r} + l\vec{p}_\omega/|\vec{p}_\omega|$  with  $\vec{r}'$  the  $\omega$  production point,  $p_\omega$  and  $\beta_\omega$  are the momentum and velocity of the  $\omega$  in the target nucleus frame, while  $\rho(r')$  stands for the local nuclear density. Eq. 11 shows that the survival probability P of the  $\omega$  meson in its way out of a nucleus decreases with increasing of the  $\omega$  width  $\Gamma^*$ .

The momentum averaged atomic mass dependence of the transparency obtained within the folding model is shown by solid curve in Fig. 4. The dashed and dash-dotted lines - which correspond to the calculations with the value of  $\Gamma^*$  multiplied by a factors of 0.5 and 2, respectively, - reflect the sensitivity of the A-dependence to the collision width  $\Gamma^*$ . The difference between the curves is large enough to be detected in the experiment. Since the shape of the A-dependence, and not so much the absolute value, is important to learn about the  $\omega$  width, the cross section for middle and heavy nuclei can be normalized to the cross section for light nucleus. The A-dependence of the transparency normalized to the cross section for the  $\omega$  production on carbon target is presented in Fig. 5. In spite of some less difference between the curves the measurement of the ratios has an advantage to cancel out most of systematic uncertainties. Thus, the calculations clearly show that the proton induced  $\omega$  meson production in nuclei can indeed be used to get information on the  $\omega$  width in the medium.

Note that the investigation of the  $\omega$  meson width and its momentum dependence in pA reactions has several important advantages as compared with one in Ap reactions. First, the proton beams are usually much more intensive than the ion ones. Second, the simple solid targets can be used instead of the hydrogen

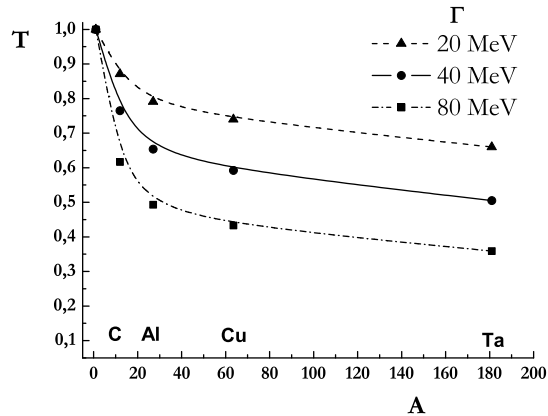


Figure 4: Transparency as a function of atomic mass number

target. Third, in the pA collisions the momentum dependence of the  $\omega$  meson width can be studied in wide momentum range from 1 up to 4 GeV/c. It is worth to note, that the possible effect of density dependent  $\omega$  meson mass shift is of minor importance in high momentum range.

## 7 Simulations with RQMD event generator

For the simulations we use Relativistic Quantum Molecular Dynamics (RQMD) [35] event generator, version 4.12, which well reproduces a number of available experimental data on pA and AA collisions. RQMD produces hadrons through the excitation of baryonic and mesonic resonances. Heavy resonances (more than 2 GeV for baryons and more than 1 GeV for mesons) are treated in the string picture following the Lund model [36] and all particles are allowed to reinteract (baryon-baryon, baryon-meson and meson-meson). The model provides a complete time-dependent description of the evolution of each event. The probabilities for excitation of specific channels are governed by experimental cross sections to the extent possible. The formation points of hadrons are taken from the properties of resonance decay and string fragmentation.

About  $3 \times 10^6$  minimum bias Cu+p events have been generated. The following simulation was performed for the ring-like electromagnetic calorimeter covering the interval of polar angles  $\theta = 5^\circ - 25^\circ$  and full azimuthal angle of  $0^\circ < \phi < 360^\circ$ . At projectile energy of 4 AGeV the mean total multiplicity is equal to 12 for Cu+p and 3.4 for C+p collisions. Multiplicities of different species are presented in Table 1. Since the charged component (protons and pions) amounts of one half

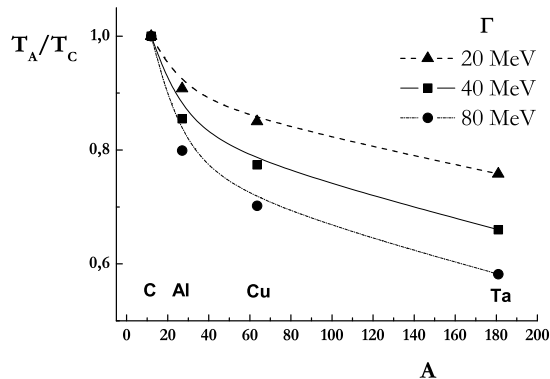


Figure 5: Transparency ratio as a function of target mass number

| species      | n   | p   | $\pi^0$ | $\pi^+$ | $\pi^-$ | $\eta$ | $\gamma$ |
|--------------|-----|-----|---------|---------|---------|--------|----------|
| multiplicity | 4.7 | 4.6 | 1.47    | 0.74    | 0.66    | 0.037  | 0.0026   |

Table 1: Mean multiplicities of particles predicted by the RQMD code for the minimum bias Cu+p events at 4 AGeV

of the total multiplicity one can estimate the impact parameter of the collision by detecting the charged ejectiles.

The angular dependence of the secondaries in the laboratory are shown in Fig. 6. It is seen that the multiplicity drops rapidly with the production angle. Due to the ring-like geometry of the EMCAL the first angular bin  $0^0 - 5^0$  is out of the detector acceptance. Assuming the target-detector distance of 1 meter and granularity of the EMCAL of  $2 \times 2 \text{ cm}^2$  one gets maximum cell occupancy of about 0.006 for minimum bias events and approximately two times more for most of central collisions in the angular bin  $5^0 - 10^0$ .

The two-dimensional plot for the  $\omega$  mesons produced in Cu+p collisions at ion beam energy of 4 AGeV is presented in the left upper panel of Fig. 7. It is seen that fast mesons in the laboratory (the target proton frame of reference) are predominantly concentrated in the range of small angles. The momentum spectrum of all produced  $\omega$ 's (right upper panel of Fig. 7) extends up to 5 GeV/c. Remind, that the  $\omega$  meson moving with the same velocity as the projectile nucleus has laboratory momentum equal to 4 GeV/c. In right upper panel of Fig. 8 we present the same laboratory spectrum with cut on the  $\omega$  meson momentum  $p < 0.5$  GeV/c in the incident nucleus rest frame. The comparison of the right upper panels of Fig. 7 and Fig. 8 shows that almost 1/4 part of all produced

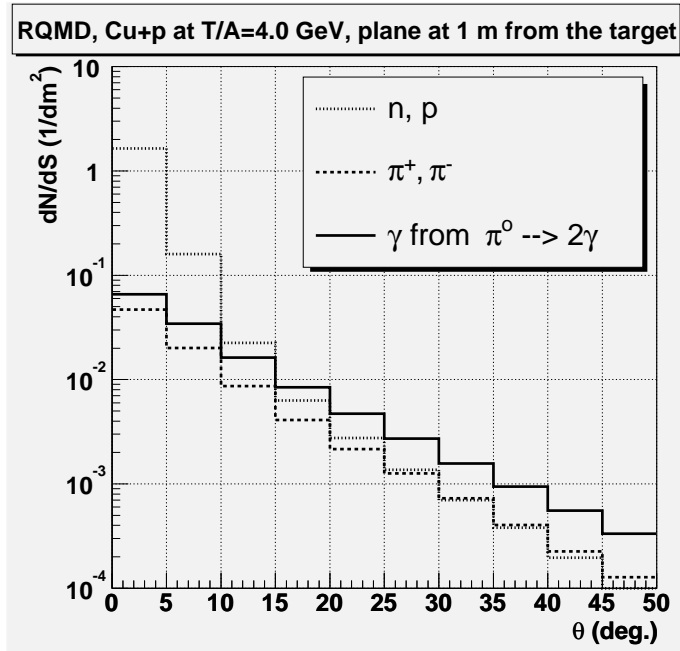


Figure 6: Density of particles in a plane at 1 m from the target

mesons are within the range  $p < 0.5$  GeV/c in the projectile Cu frame of reference. In the right bottom panels of Fig. 7 and Fig. 8 the two-dimensional distributions - rapidity versus transverse momentum - are presented without and with the above cut on the  $\omega$  momentum, respectively. One can see the sizeable number of events with small  $p_t$  in the vicinity of the projectile nucleus rapidity  $Y=2.34$  in the laboratory system. The most of  $\omega$ 's have the rapidities  $Y < 2.34$  and show up at  $Y < 0$  in the projectile nucleus rest frame (bottom right panel of Fig. 9). Thus, the range of low  $p_t$  and very small and even zero rapidities is accessible for the investigation in Ap kinematics. As was above mentioned the real part of the  $\omega$  meson-nuclear potential probably depends on the  $\omega$  momentum relative to the nuclear medium. The most strong effect is expected for the momenta of less than 0.3 GeV/c. The study of the  $\omega$  meson invariant mass distributions reconstructed for different momentum bins in the range of  $P_\omega < 0.5$  GeV/c provides the possibility to explore the momentum dependence of the  $\omega$  mesons mass shift in the medium.

In principle, the same spectrum can also be measured in pA reaction using the  $4\pi$  detector with high resolution for low energy photons. However, the use of the inverse kinematics is much more effective way to collect all produced low momentum mesons and detect much more energetic photons from their decays by compact EMCAL. Indeed, the left upper panel of Fig. 8 shows that about 800  $\omega$  mesons with momenta of less than 0.5 GeV/c relative to the projectile nucleus

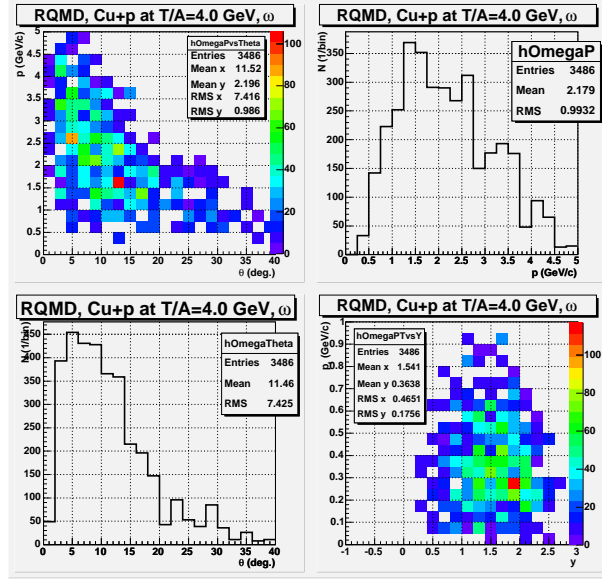


Figure 7:  $\omega$  spectrum in the laboratory frame

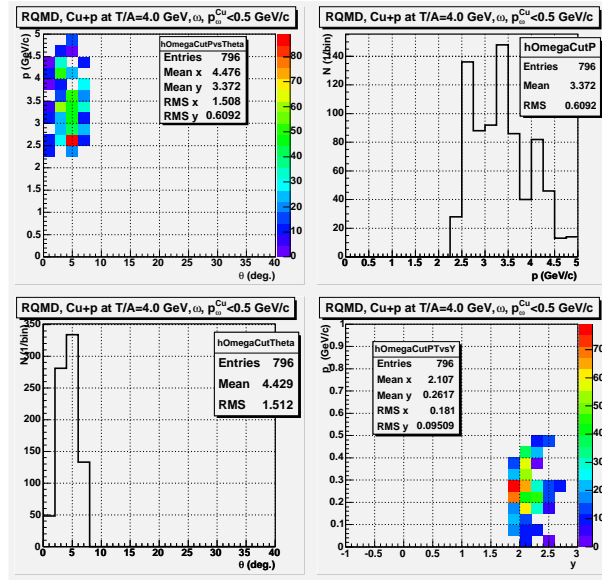


Figure 8: The same as for Fig. 7 but for  $\omega$  with  $p < 0.5$  GeV/c in the projectile nucleus frame

are within the cone of 10 degrees in the case of Ap collisions while only about 10  $\omega$  mesons are in the same momentum and angular range in the case of pA collisions ( $p < 0.5 \text{ GeV}/c$  in the first angular bin in the left upper panel of Fig. 9). Such a relation is in accordance with one following from Eq. 5.

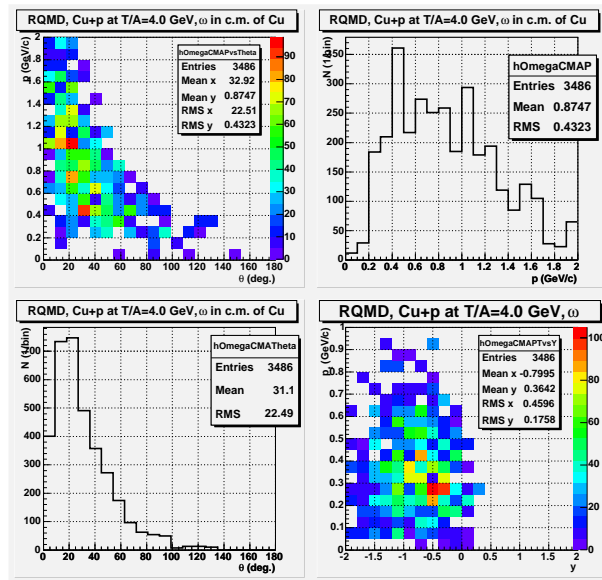


Figure 9:  $\omega$  spectrum in the projectile nucleus frame

For the selection of useful events the EMCAL should be able to detect efficiently three photons from the  $\omega \rightarrow \pi^0 \gamma \rightarrow 3\gamma$  decay. The performed simulations show that the geometrical efficiency for the detection of the photons from the  $\omega$  decay is near 40 % for the range of small production angles ( $\theta < 7.5^\circ$ ) and high  $\omega$  momentum ( $p > 2.25 \text{ GeV}/c$ ) in the laboratory which corresponds to the range of  $p_\omega < 0.5 \text{ GeV}/c$  in the projectile nucleus rest frame. Since invariant mass resolution decreases with lowering of the photon energy, we have determined the efficiency after applying the cut on  $E_\gamma > 0.5 \text{ GeV}$ . It amounts to about 15-20% in the range of our interest. The simulations indicate that the detection efficiency of low momentum  $\omega$  mesons produced in Ap collisions turns out approximately 10 times higher than that averaged over all meson momenta.

As was explained in section 6.2 the in-medium  $\omega$  meson width can be deduced from the analysis of the A-dependence of the production cross sections of relatively fast  $\omega$ 's, which are mostly decaying outside the nucleus. Obviously, that the photons from the decay of high momentum mesons produced in traditional pA kinematics will be detected with the same efficiency because the efficiency depends on their energy relative to the detector. Thus, the momentum dependencies of both in-medium  $\omega$  meson mass and width can be investigated using

the inverse and direct kinematics – i.e. the ion and proton beams – without the change of the detector position and its layout.

## 8 Background and its suppression

The feasibility of the experiment depends on the signal to background ratio. RQMD simulations show that the main source of the background is the  $\pi^0\pi^0$  production. Such of events can lead to the misidentification due to a finite geometry of the detector if one of the four photons is out of the EMCAL acceptance. The contribution from other sources of the background like  $\eta\pi^0$ ,  $\eta'$ ,  $\Delta^0 \rightarrow n\gamma$  etc. is relatively small in the invariant mass range of interest 0.65 - 0.85 GeV since the invariant masses reconstructed from kinematical parameters of three uncorrelated photons are spread over wide mass range from 0.1 to 1.0 GeV. Therefore, the useful events from the  $\omega \rightarrow \pi^0\gamma \rightarrow 3\gamma$  decay will be detected on the top of smooth continuum steaming mainly from the  $\pi^0\pi^0$  production process. The Signal/(Signal+Background) ratio  $R = S/(S + B)$  for the minimum bias events is less than approximately one per cent. However, this value can be significantly improved by applying the appropriate kinematical cuts. RQMD simulations indicate that the spectrum of the photons originating from the  $\pi^0$  decay drops more steep than that from the  $\omega$  decay. By this reason the cut on photon energy should lead to the background suppression.

The histograms in Fig. 10 demonstrate this effect. Invariant mass distributions of  $\pi^0\gamma$  system without the cut on photon energies are shown in the upper row, while the middle and bottom rows represent the distributions obtained with cuts on  $E_\gamma > 0.5$  GeV and  $E_\gamma > 1$  GeV, correspondingly. The mass distributions from RQMD simulations are presented in the left column. In the right column the same distributions are depicted for the case when the energy and space resolution of the PbWO calorimeters are taken into account. The numbers of the signal (S) and signal plus background (S+B) events are collected in Table 2. The magnitude of  $R=21\%$  and mass resolution of 12 MeV can be reached after implying the cut on a photon energy  $E_\gamma > 1$  GeV. However, it is accompanied by the reduction of signal events by a factor of 8 compared to one for the case  $E_\gamma > 0.5$  GeV.

The discussed Signal/(Signal+Background) ratio can be even further improved since the  $\pi^0$  and  $\gamma$  which are, in fact, from the  $\omega$  decay are strongly correlated while the photons steaming from the  $\pi^0\pi^0$  or other sources will not show such a correlation. Remind that the use of the inverse kinematics results in the production picture in which slow  $\omega$  mesons in the projectile nucleus rest frame are predominantly produced close to the beam direction in the laboratory. Due to two-body nature of the  $\omega \rightarrow \pi^0\gamma$  decay the pion should be emitted in the plane which is formed by the projectile momentum and the momentum of the photon originated from the  $\omega$  decay. In such a case the difference in the azimuthal

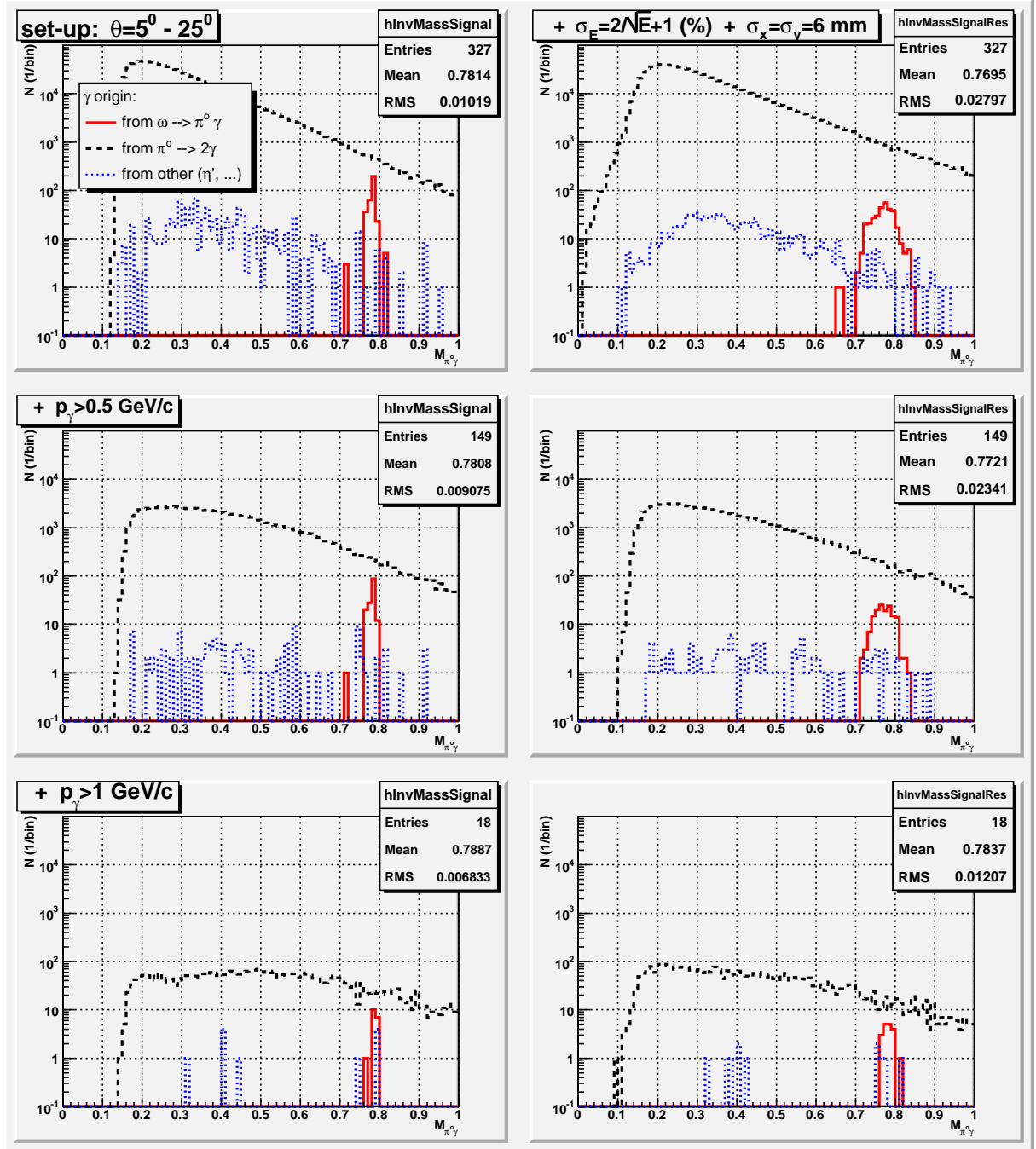


Figure 10: Invariant mass spectra with and without cuts on the photon energies

| EMCAL             | info                  | all                        | $E_\gamma > 0.5\text{GeV}$ | $E_\gamma > 1\text{GeV}$ |
|-------------------|-----------------------|----------------------------|----------------------------|--------------------------|
| without<br>resol. | S/(S+B)<br>RMS(S) MeV | 327/(327+3130)=9.5%<br>10  | 149/(149+1267)=10.5%<br>9  | 18/(18+67)=21%<br>7      |
| PbWO<br>resol.    | S/(S+B)<br>RMS(S) MeV | 323/(323+17689)=1.8%<br>28 | 149/(149+2398)=5.9%<br>23  | 18/(18+68)=21%<br>12     |

Table 2: Parameters of signal (S) and background (B)  $\pi^0\gamma$  pairs

angles of the  $\pi^0$  and  $\gamma$  is close to 180 degrees. The cut  $\phi_\pi - \phi_\gamma > 100^\circ$  results in additional increase of R by a factor of 2.

Thus, we conclude that the applying of the appropriate cuts permit to reduce the background to the level acceptable for the measurements.

## 9 Event trigger

The events of interest detected by EMCAL are accompanied by the deposit of energy in three or more groups of cells. For the selection of such events a multilevel trigger could be used. A first level should be provided by the signals selected the events with energy deposit of more than 0.5 GeV for the suppression of background from low momentum  $\pi^0$  production and their rescattering. The second level of the trigger would include the requirement the energy deposit of more than 1 GeV in one of the cell group which correspond to the photon energy from the real  $\omega$  meson decay. The third level would select the events with large azimuthal separation corresponding to actual two-body  $\omega$  decays. One can estimate a contribution of background events using the experimental counting statistics of the inclusive trigger and the trigger of delayed coincidence. The information from veto counters will be used as an off-line trigger for the reduction of charged background and for the estimation of the collision centrality.

## 10 Event rate estimate

Let us first estimate the expected number of events for the production of low momentum mesons with respect to a projectile nucleus. The momentum spectrum of the  $\omega$  mesons from the  $3 \times 10^6$  Cu + p collisions at initial energy of 4 AGeV obtained from the RQMD simulations is presented at the histogram in the right upper panel of Fig. 9. Assuming a moderate ion beam intensity of  $1 \times 10^8$  ions/cycle, the extraction efficiency of 50% and target efficiency of 2% one gets the number of the ion interactions inside the target of  $1 \times 10^6$  per one accelerator cycle. The normalization factor  $N$  - which is the ratio of the number of interaction during one accelerator cycle to the number of simulated collisions - is equal

to 0.33. The momentum intervals of less than 0.3 GeV/c and 0.5 GeV/c contain 225 and 796 events, respectively (see right top histogram in Fig. 9).

Assuming the cycle repetition of  $10 \text{ min}^{-1}$  and taking into account the detector efficiency of 15% (after applying the cut on  $E_\gamma > 0.5 \text{ GeV}$ ) one can estimate the event rate for the above momentum ranges as:

$$N(P_\omega < 0.3 \text{ GeV/c}) = 0.33 \times 225 \times 0.15 \times 10 = 111 \text{ events/min}$$

$$N(P_\omega < 0.5 \text{ GeV/c}) = 0.33 \times 796 \times 0.15 \times 10 = 398 \text{ events/min.}$$

As was described in the section 8 one has to apply several cuts to reach the background conditions acceptable for the measurements. That leads to the reduction of useful events by a factor of 10-20. In the most pessimistic case the numbers of useful events collected during one day measurement are:

$$N(P_\omega < 0.3 \text{ GeV/c}) = 8 \times 10^3 \text{ events/day}$$

$$N(P_\omega < 0.5 \text{ GeV/c}) = 28.6 \times 10^3 \text{ events/day}$$

The number of events in the lowest momentum interval  $P_\omega < 0.1 \text{ GeV/c}$  is equal to approximately 400 per day. For the carbon projectile the event rates will be less by a factor of 4-5 due to the A-dependence of the production cross section. Thus, the estimate clearly demonstrates that the investigation of the momentum dependence of the expected  $\omega$  meson mass shift in the nuclear matter can be performed with high statistical accuracy.

It should be noted that the above estimates are based on the RQMD simulations which disregard any medium effects on the  $\omega$ . If the  $\omega$  meson mass really drops in nuclear matter by 80-100 MeV the production cross section would increase due to the downward shift of the reaction threshold. Moreover, one can expect that the produced mesons will be decelerated during their way out of the nucleus due to the action of the attractive nuclear  $\omega$  meson potential. This slowing down would lead to the increase in number of events in low momentum range. Note also that the energy loss of a meson in the elastic and quasielastic  $\omega N$  scattering inside a nucleus results in the same effect.

The use of more intensive proton beam provides the possibility to collect large amount of data on high momentum  $\omega$  mesons production and perform the detail investigation of the momentum dependence of the  $\omega$  meson width in the nuclear matter. Data on the  $\omega$  meson production in the momentum range around 1.5 GeV/c can be obtained in both inverse and direct kinematics. These data will be used for the cross check and mutual normalization of the Ap and pA measurements. The statistics which can be obtained in AA interactions is obviously higher than that in Ap(pA) collisions.

## 11 Conclusion

The modification of the properties of the vector mesons in baryon environment continue to be one of the most interesting topics in hadron physics today.

We suggest to investigate the in-medium properties of the  $\omega$  mesons at normal

nuclear density in nucleus-proton and proton-nucleus collisions as well as at higher density in nucleus-nucleus collisions at ITEP accelerator facility TWAC.

Study of the Ap and pA reactions is the effective tool to learn about the in-medium  $\omega$  meson properties at normal nuclear density.

The using of the inverse Ap kinematics and  $\omega \rightarrow \pi^0\gamma$  decay mode permits us to collect large statistics for production of the  $\omega$  mesons with low momenta relative to the nuclear matter. Estimated high event rate offers the possibility to split the statistics into several momentum bins and study the  $\omega$  meson mass shift in wide momentum interval *including not yet explored range of momentum less than 0.3 GeV/c which is expected to be most sensitive to the mass change effect*. The detail information on the momentum dependence of the in-medium  $\omega$  meson width will be obtained in pA collisions.

The goal of the first stage of the experiment is to make decisive conclusion about the in-medium  $\omega$  meson mass and width at normal nuclear density.

On the second stage of the suggested study we shall obtain the information on the  $\omega$  meson production in nucleus-nucleus collisions which will be used for the investigation of the in-medium  $\omega$  meson properties at higher density compared to that accessible in nucleus-proton interactions. The results obtained at the first stage of the investigation at normal nuclear density will provide the reliable basis for the selection and interpretation of specific nucleus-nucleus phenomena.

Ap, pA and AA measurements will be performed in identical conditions using the same experimental set-up.

## 12 Further investigations at ITEP and GSI

One of the possible extension of the proposed studies in a few GeV energy range is the investigation of the in-medium change of pseudoscalar mesons. The performed RQMD simulations of the Ap collisions show the significant yield of the  $\eta$  and  $\eta'$  mesons for which the modification effects had also been theoretically predicted [37], [5]. The branching ratios of the  $\eta \rightarrow \gamma\gamma$  and  $\eta' \rightarrow \pi_0\pi_0\gamma\gamma$  decays are as high as 39% and 21%, correspondingly. The properties of these mesons can be investigated at TWAC using the same experimental set-up.

The in-medium properties of the antikaons have captured the attention of hadron community. As it was predicted by Akaishi and Yamazaki [38] an  $\bar{K}$  feels strong attraction in matter leading to the formation of narrow deeply bound nuclear kaonic states and a shrinkage effect on nuclear environment turns out in an increase of the average density up to 3-4 times the normal value. Some experimental indications on the formation of  $K^-$ -nucleus states have been recently obtained at DAFNE(FINUDA) [39] and BNL-AGS(E930) [40]. The scientific program of recently formed AMADEUS collaboration aimed at the *"precision spectroscopy studies of a number of light kaonic nuclei and study the quark condensates at large quark density"* (LOI, March 2006). The proton and ion beams

of the ITEP-TWAC facility offer the possibility to investigate the in-medium antikaon and kaon properties in Ap(pA) and AA collisions in the energy range of 2 - 4 AGeV.

The in-medium properties of the charmed mesons and charmonium can be explored at significantly higher ion energy which will be accessible at the new FAIR facility (GSI). In particular, the mass splitting of  $\bar{D}D$  at high baryonic density [41] will be investigated by CBM experiment in heavy-ion collisions. As a masses of charmonia are large, only little sensitivity to changes in the quark condensate is expected. Consequently, the in-medium mass of the charmonium states would be affected primary by a modification of the gluon condensate. Large attractive mass shifts are predicted for excited charmonium states [42]. Using the inverse and direct kinematics provides the possibility to study the production and propagation of both low and high momentum heavy quark systems in baryonic matter.

## 13 Acknowledgments

We authors gratefully acknowledge N.O.Agasian, B.L.Ioffe, L.A.Kondratuyk for fruitful discussions. This work was partially supported by Federal agency of Russia for atomic energy (Rosatom).

— **The suggested investigation is open for the cooperation with the experimentalists and theorists who are interested in the above discussed physics and in the performing of the proposed experiment.**

## References

- [1] T. Hatsuda and S.H. Lee, Phys. Rev. **C46**, R34 (1992).
- [2] G.E. Brown and M. Rho, Phys. Rev. Lett. **66**, 2720 (1991).
- [3] P.S. Reinhard, Rep. Prog. Phys. **52**, 439 (1989).
- [4] T. Tsushima *et al.*, Phys. Lett. **B429**, 239 (1998).
- [5] K. Saito *et al.*, Prog. Part. Nucl. Phys. **58**, 1 (2007).
- [6] S. Leupold, Nucl. Phys. **A628**, 311 (1998).
- [7] K. Suzuki *et al.*, Phys. Rev. Lett. **92**, 072302 (2004).
- [8] Y. Nambu and G. Jona-Lasino, Phys. Rev. **122**, 345 (1961).
- [9] S. Zschocke *et al.*, Phys. Lett. **B562**, 57 (2003); R. Tomas *et al.*, Phys. Rev. Lett. **95**, 232301 (2005).

- [10] G. Agakichiev *et al.*, Phys. Lett. **B422**, 405 (1998).
- [11] J. Adams *et al.*, Phys. Rev. Lett. **92**, 092301 (2004).
- [12] W. Weise, Nucl. Phys. **A610**, 35c (1996).
- [13] U. Mosel, Pramana **66**, 709 (2006).
- [14] D. Trnka *et al.*, Phys. Rev. Lett. **94**, 192303 (2005).
- [15] M. Naruki *et al.*, Phys. Rev. Lett. **96**, 092301 (2006).
- [16] M. Kaskulov *et al.*, Eur. Phys. J. **A31**, 245 (2007), arXiv:nucl-th/0610067.
- [17] C. Djalali for the CLAS Collaboration, Proceedings of the QM'2006 Conference, China, November 2006.
- [18] M. Kotulla, arXiv: nucl-ex/0609012.
- [19] B. Yu. Sharkov *et al.*, Nucl. Instr. Meth. **A415**, 20 (1998).
- [20] D. Cabrera *et al.*, Nucl. Phys. **A733**, 130 (2004).
- [21] K. Tsushima *et al.*, Phys. Lett. **B433**, 26 (1998); F. Klingl *et al.*, Nucl. Phys. **A624**, 527 (1997); B. Friman, Acta Phys. Pol. **B29**, 3115 (1998); K. Saito *et al.*, Phys. Lett. **B433**, 243 (1998); K. Saito *et al.*, Phys. Rev. **C59**, 1203 (1999); F. Klingl *et al.*, Nucl. Phys. **A650**, 299 (1999);
- [22] A.K. Dutt-Mazumder *et al.*, Phys. Rev. **C63**, 015204 (2001); M. Post and U. Mosel Nucl. Phys. **A669**, 169 (2002); B. Stainmueller and S. Leupold Nucl. Phys. **A778**, 195 (2006);
- [23] M. F. M. Lutz *et al.*, Nucl. Phys. **A706**, 431 (2002); P. Muehlich *et al.*, Nucl. Phys. **A780**, 187 (2006);
- [24] F. Klingl *et al.*, Nucl. Phys. **A624**, 527 (1997); B. Friman, Acta Phys. Pol. **B29**, 3115 (1998);
- [25] P. Muehlich *et al.*, Eur. Phys. J. **A20**, 499 (2004).
- [26] J. G. Messchendorp *et al.*, Eur. Phys. J. **A11**, 95 (2001).
- [27] Yu. Kiselev and V. Sheinkman, JETP Lett. **78**, 528 (2003).
- [28] A.V. Akindinov *et al.*, JETP Lett. **72**, 100 (2000).
- [29] R. S. Hayano *et al.*, Eur. Phys. J. **A6**, 99 (1999); F. Klingl *et al.*, Nucl. Phys. **A650**, 299 (1999);

- [30] P. Muehlich and U. Mosel Nucl. Phys. **A773**, 156 (2006).
- [31] P. Muehlich *et al.*, Phys. Rev. **C67**, 024605 (2003).
- [32] G. I. Lykasov *et al.*, Eur. Phys. J. **A6**, 71 (1999).
- [33] T. Ishikawa *et al.*, Phys. Lett. **B608**, 215 (2005).
- [34] V. K. Magas *et al.*, Phys. Rev. **C71**, 065202 (2005).
- [35] H. Sorge, H. Stöcker and W. Greiner, Ann. Phys. (NY) **192**, 266 (1989); Nucl. Phys. **A498**, 567c (1989); Z.Phys. **C47**, 629 (1990); H. Sorge, Phys. Rev. **C52**, 3291 (1995).
- [36] B. Nilsson-Almqvist and E. Stenlund, Computer Phys. Comm. **43**, 387 (1987); B. Andersson, G. Gustafson and B Nilsson-Almqvist, Nucl. Phys. **B281**, 289 (1987).
- [37] H. Hagahiro *et al.*, Phys. Rev. **C74**, 045203 (2006).
- [38] Y. Akaishi and T. Yamazaki Phys. Rev. **C65**, 044005 (2002).
- [39] M. Agnello *et al.*, Phys. Rev. Lett. **94**, 212303 (2005).
- [40] T. Kishimoto *et al.*, Nucl. Phys. **A754**, 383c (2005).
- [41] A. Sibirtsev *et al.*, Eur. Phys. J. **A6**,351 (1999); A.Hayashigaki Phys. Lett. **B487**, 96 (2000); L. Tolos *et al.*, Phys. Rev. **B635**, 85 (2006).
- [42] S. Lee and C. Ko Phys. Rev. **C67**, 038202 (2003).